



**Calhoun: The NPS Institutional Archive**  
**DSpace Repository**

---

Faculty and Researchers

Faculty and Researchers' Publications

---

2020

# Astrobatomics: Characterization of Experimental Self-Toss Maneuvers at the Naval Postgraduate School and NASA Ames

Choon, Stephen Kwok; Safbom, Conor; Chitwood, Jonathan; Leary, Patrick; Summerlin, James; Watanabe, Daniel; Barlow, Jonathan; Romano, Marcello

AAS

---

Choon, Stephen T. Kwok, et al. "Astrobatomics: Characterization of Experimental Self-Toss Maneuvers at the Naval Postgraduate School and NASA Ames." *Advances in the Astronautical Sciences*, Vol 175, 2020.

<http://hdl.handle.net/10945/70558>

---

This publication is a work of the U.S. Government as defined in Title 17. United



*Downloaded from NPS Archive: Calhoun*

Calhoun is the Naval Postgraduate School's public access digital repository for research materials and institutional publications created by the NPS community.

Calhoun is named for Professor of Mathematics Guy K. Calhoun, NPS's first appointed -- and published -- scholarly author.

**Dudley Knox Library / Naval Postgraduate School**  
**411 Dyer Road / 1 University Circle**  
**Monterey, California USA 93943**

<http://www.nps.edu/library>

# ASTROBATICS: CHARACTERIZATION OF EXPERIMENTAL SELF-TOSS MANEUVERS AT THE NAVAL POSTGRADUATE SCHOOL AND NASA AMES

**Stephen Kwok Choon,<sup>\*</sup> Conor Safbom,<sup>†</sup> Jonathan Chitwood,<sup>†</sup> Patrick Leary,<sup>†</sup> James Summerlin,<sup>†</sup> Daniel Watanabe,<sup>†</sup> Jonathan Barlow,<sup>‡</sup> and Marcello Romano<sup>§</sup>**

Astrobee is a small, compact vehicle designed to operate onboard the International Space Station and perform tasks related to observation, maintenance, and hosting guest science experiments. ASTROBATICS, is an experiment led by the Spacecraft Robotics Laboratory of the Naval Postgraduate School in collaboration with NASA. ASTROBATICS is investigating self-toss hopping maneuvers to be utilized within the International Space Station in order to provide a method of locomotion. As part of the preliminary preparation, experiments were conducted at the Naval Postgraduate School and NASA Ames in order to characterize self-toss maneuvers.

## INTRODUCTION

The utilization of self-toss maneuvers for on-orbit robotic vehicles as a method of locomotion is explored in preparation of experiments onboard the International Space Station (ISS)<sup>1</sup>. The characterization of the Astrobee robotic arm is performed on the Floating Spacecraft Simulator (FSS) Testbeds at the Naval Postgraduate School (NPS) and NASA Ames Research Center. The experiments involve the actuation of the respective proximal and distal robotic arm joint from a prescribed initial start angle to a given final end angle followed by gripper release. This series of experiments is intended to provide preliminary understanding of the dynamic behavior of Astrobee and the desired actuation parameters for performing self-toss maneuvers that can then be compared to Astrobee self-toss maneuvers onboard the ISS. Allowing for better path-planning and knowledge about the dynamic motion and interaction of Astrobee with its environment during the self-toss maneuver.

Hopping maneuvers as a method of locomotion has been studied for both terrestrial<sup>2</sup> and space vehicles<sup>3,4</sup>. Low gravity and uneven terrain in space impose mobility challenges for conventional robots, hopping can provide a solution by jumping over uneven terrain surfaces<sup>5-8</sup>. Hopping as a method for maneuvering was utilized on an asteroid surface mission with MINERVA<sup>9</sup> on Hayabusa

---

<sup>\*</sup> NRC Postdoctoral Research Associate, MAE, Naval Postgraduate School, 1 University Circle, Monterey, CA 93943

<sup>†</sup> Graduate Student, MAE, Naval Postgraduate School, 1 University Circle Monterey, CA 93943.

<sup>‡</sup> Senior Aerospace Research Engineer, NASA Ames Research Center, KBR, Inc., Mail Stop 269-1 Bldg. 269 Rm. 260-25 P.O. Box 1 Moffett Field, CA, 94035.

<sup>§</sup> Professor, MAE, Naval Postgraduate School, 1 University Circle Monterey, CA 93943.

I & II by JAXA.<sup>\*†10</sup> The utilization of hopping maneuvers by robots such as Astrobee on-board the ISS could provide a useful method of locomotion, and is thus explored.

This paper is presented in five sections. First, a description of Astrobee is provided as well as the robotic arm module that was used at NPS. Second, the Floating Spacecraft Simulators (FSS) at NPS and NASA Ames that shall be used to perform the experiments at each respective facility are described. Third, a description of the experimental procedures for both the Proximal and Distal experiments are discussed, with the prescribed actuator joint limitations as well sequence of actions that are intended to be performed. Fourth, a discussion of results from self-toss maneuvers performed at NPS and Ames, with the intention that additional experimental testing shall occur. Lastly, an outline and conclusion based on the results collected from experiments performed at NPS and NASA Ames is presented.

## ASTROBEE ROBOTIC ARM MODULE

Astrobee is free-flyer equipped with a manipulator perching arm, as well as an array of sensors as shown in Figure 1 where described there are the SciCam, NavCam, HazCam, PerchCam, and DockCam, flashlight, microphone, air intake impellers, as well as twelve nozzles to provide thrust and navigation.. Examples of previous free-flyers that have been launched on-board the ISS include SPHERES<sup>11</sup>, Int-Ball<sup>12</sup>, and CIMON<sup>13</sup>. Astrobee is designed to support and alleviate crew activities by performing tasks that are routine, repetitive, simple but long duration such as conducting environment surveys, taking sensor readings, as well as monitoring crew activities and guest science applications.<sup>14-17,‡</sup>

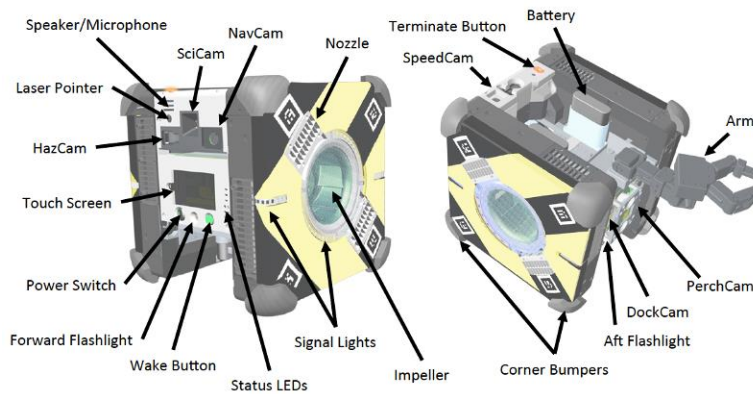


**Figure 1: Astrobee Schematic Highlighting Key Features**<sup>14,18</sup>

The Self-Toss maneuver has been divided into three main sections from the initial push, free-coast flying, to the required soft-landing.<sup>1,19,20</sup> Shown in Figure 2 is the Three Degree-Of-Freedom Astrobee robotic perching arm module. The robotic arm is composed of a base, proximal joint, distal joint, and gripper end-effector. Each joint of the perching arm was commanded to actuate at

\* <https://www.space.com/41941-hayabusa2-asteroid-rovers-hopping-tech.html>

† [https://global.jaxa.jp/article/special/hayabusa/index\\_e.html](https://global.jaxa.jp/article/special/hayabusa/index_e.html)

‡ <https://www.nasa.gov/feature/ames/nasa-s-new-flying-robots-bee-ing-in-space-for-the-first-time>

a constant angular rate of  $0.12 \text{ rad/s}^*$ , from the Dynamixel XH430-210 actuator datasheet<sup>†</sup> the amount of torque provided is approximately 1.70 Nm.

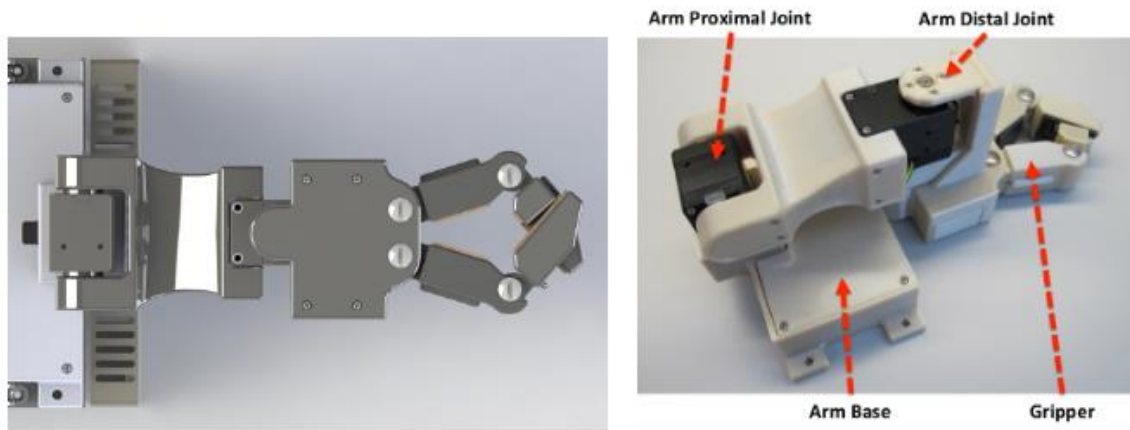


**Figure 2: Astrobee Robotic Arm: Shown is the Proximal and Distal Joint<sup>20,21</sup>**

### EXPERIMENTAL SET-UP AT NPS AND AMES

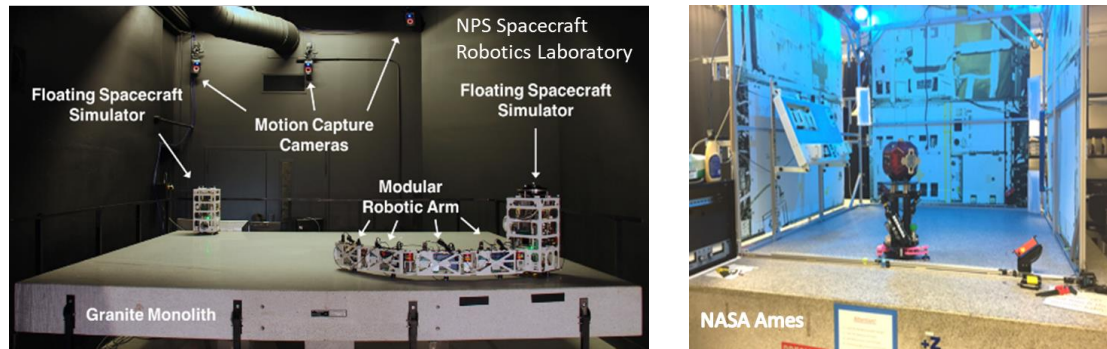


**Figure 3: Floating Testbed Simulators at NPS (Left)<sup>22,23</sup> and NASA Ames Research Center (Right)<sup>‡</sup>**

The experimental set-up is depicted in Figure 3 with the Floating Testbed Simulators of NPS (left) and the NASA Ames Research Center (right). The Proximity Operation of Spacecraft: Experimental hardware-In-the-loop DYNAMIC simulator (POSEIDYN)<sup>22,24</sup> at the Naval Postgraduate School consists of a 4 x 4 m granite table, multiple Floating Spacecraft Simulators (FSS) and a commercial navigation sensor, VICON, comprised of ten-camera array to track retro-reflective markers located on the FSS. The Floating Testbed Simulator at NASA Ames Research Center is composed of a granite table, with the ability to potentially operate two Astrobee vehicles on its surface at the same time with three Degree-of-Freedom planar motion.

The Astrobee Free-Flyer Vehicle at the NASA Ames Research Center is shown on the left in Figure 4. In this figure, Astrobee has its robotic arm in the stowed configuration located on a stand that utilizes three air-bearing pads and compressed air to provide frictionless three Degree-of-

\*<https://github.com/nasa/astrobee/blob/70e3df03ff3f880d302812111d0107f3c14dccc0/description/description/urdf/model.urdf.xacro>

† [http://support.robotis.com/en/product/actuator/dynamixel\\_x/xh\\_series/xh430-w210\\_main.htm](http://support.robotis.com/en/product/actuator/dynamixel_x/xh_series/xh430-w210_main.htm)

‡ <https://www.nasa.gov/content/spheresastrobee-working-group>

Freedom motion. Figure 4 on the right, displays the NPS FSS vehicle with the replica Astrobeer Robotic Arm module mounted to its front. The FSS at NPS has allowed for rapid testing and experimentation of self-toss maneuvers using the Astrobeer Robotic Arm.

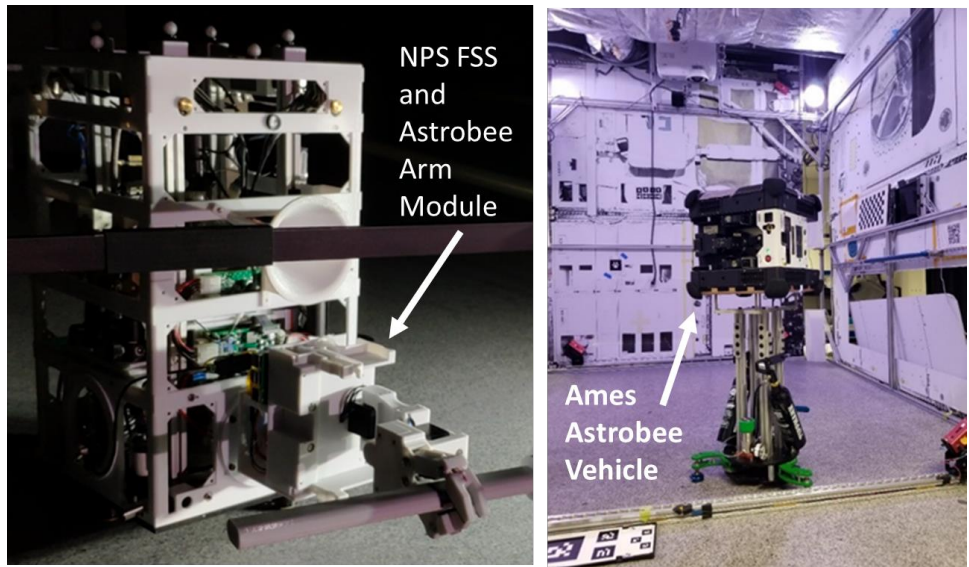


**Figure 4: NPS FSS and NPS Astrobeer Arm Module (Left), and Ames Astrobeer Vehicle (Right)**

## EXPERIMENTAL PROCEDURE – Self-Toss Maneuver

### Astrobeer Joint Operation Limits

The proximal and distal joint of the Astrobeer robotic arm joint coordinate frames are shown in Figure 5. Whereby as defined by the Astrobeer Command Dictionary, \* the proximal joint, Tilt, has a commanded actuation limitation of  $[+90, -30]$  degrees, with the Distal Joint, Pan, having a limitation of  $[+90, -90]$  degrees. The actuation limits allow for safe operation and prevent inadvertent damage to the Astrobeer vehicle from the Robotic Arm during operation.

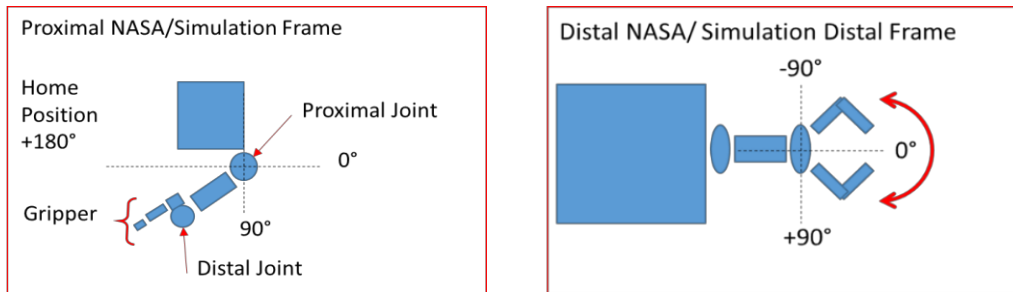


**Figure 5: Coordinate Frame of the Astrobeer Robotic Proximal (left) and Distal (Right) Joint**

### Experimental Test Sequence





From Table 1, a sequence of Self-Toss experiments was performed during the experimental session with Astrobeer. At NASA Ames and NPS each case was intended to be repeated at a

\* <https://github.com/nasa/astrobeer/wiki/Command-Dictionary>

minimum of three run, with the proximal cases performed at both facilities shown in green, with the cases performed at NPS in orange, with invalid cases in red, and the cases outside the current scope of experimental testing in hashed red lines. Additional further experimental testing with the Astrobee free-flyer at NASA Ames were scheduled but unfortunately delayed.

**Table 1: Series of Experiments performed at NPS and Ames**

		Final Proximal Goal (°)						
		0	15	30	45	60	75	90
Initial Proximal Angle (°)	30	Outside Scope	NPS	N/A	NPS	NPS	NPS	Outside Scope
	45	Outside Scope	NPS	NPS	N/A	NPS & Ames	NPS & Ames	Outside Scope
	60	Outside Scope	NPS	NPS	NPS	N/A	NPS	Outside Scope
		Final Proximal Goal (°)						
		60	75	90	105	120		
Initial Proximal Angle (°)	45	Outside Scope	NPS & Ames	NPS & Ames	NPS & Ames	NPS & Ames	Outside Scope	
	90	Outside Scope	NPS & Ames	N/A	NPS & Ames	NPS & Ames	Outside Scope	
	135	Outside Scope	NPS & Ames	NPS & Ames	NPS & Ames	NPS & Ames	Outside Scope	
		Final Distal Goal (°)						
		-45	-30	-15	0	15	30	45
Initial Distal Angle (°)	45	Outside Scope	NPS	NPS	N/A	NPS	NPS	Outside Scope
	0	Outside Scope	NPS	NPS	N/A	NPS	NPS	Outside Scope
	-45	Outside Scope	NPS	NPS	N/A	NPS	NPS	Outside Scope

Legend	
	NPS
	NPS & Ames
	N/A
	Outside Scope

## RESULTS

### NPS Self-Toss Proximal Experiment

An example of a proximal self-toss maneuver performed at NPS of the FSS and Astrobee Robotic Arm Module is shown in Figure 6. The FSS starts at the grasped position on the handrail, then a command is executed to actuate the proximal joint, where upon reaching the final joint angle the end-effector is then commanded to release allowing the FSS to perform the self-toss maneuver.

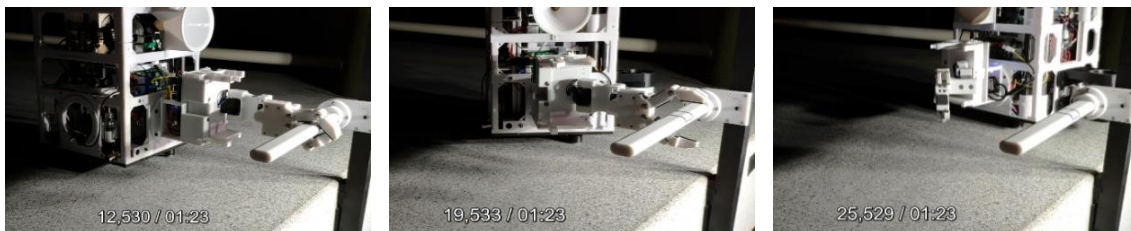


**Figure 6: Example A, Proximal Self-Toss Maneuver at NPS from horizontal handrail**

Figure 7 depicts a case (45 deg  $\rightarrow$  75 deg) which is composed of three runs from an initial proximal start angle of 45 to 75 degrees. In the plot, the start position of the self-toss maneuver is with the FSS grasping onto the horizontal hand rail. The trajectory of the corresponding three runs

were plotted as well as a depiction of the orientation and position of the FSS and the Astrobee Arm Module.

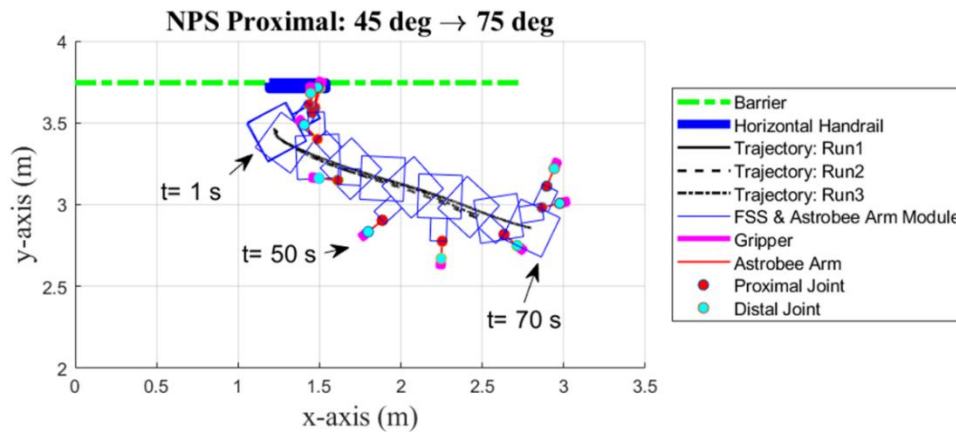


**Figure 7: Graph of Proximal Self-Toss Maneuver from Initial Angle 45 → 75 Degrees**

Figure 8 shows the FSS state information  $[x, y, \phi]$  to allow for a comparison of the dynamic motion of the vehicle for each run of the same case during the self-toss maneuver. Whereby the FSS vehicle starts at rest, then at the 20 second mark the proximal joint is actuated. This causes the vehicle to displace in the x and y-direction, with the heading of the vehicle,  $\phi$ , changing at a constant rate.

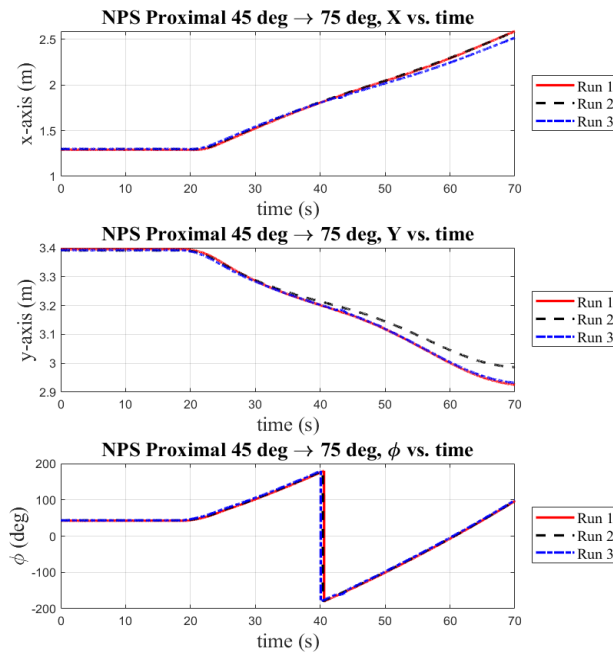


**Figure 8:  $[x, y, \phi]$  of the FSS during the Self-Toss Proximal Maneuver 45 → 75 degrees**

## NPS Proximal Experiments

The NPS proximal experiments are depicted in Figure 9 - Figure 14. A comparison of the dynamic motion of the vehicle during the maneuver based on the final angle during actuation and the subsequent release of the end effector gripper from the handrail.

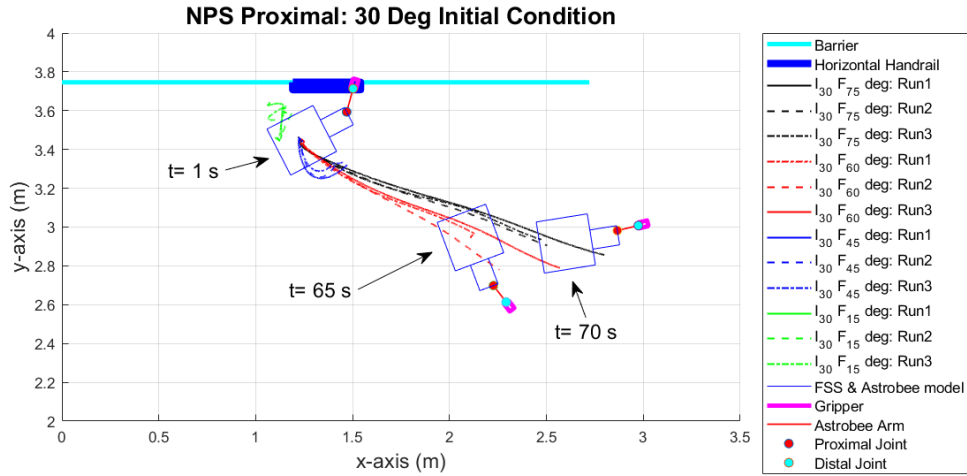


Figure 9:  $NPS_{Prox}I_{30}F_{15,45,60,75}$ , Initial 30 deg to Final Angle: 15, 45, 60, and 75 deg

Figure 9 the NPS proximal self-toss maneuver from Initial angle 30 degrees to Final angle 60 degrees ( $NPS_{Prox}I_{30}F_{60}$ ) is displayed by the set of red solid and dashed lines. Whereby from the initial start angle of 30 degrees the trajectories of  $NPS_{Prox}I_{30}F_{60,75}$  depict a successful self-toss maneuver. Similarly, from Figure 10 the trajectory of the three runs of  $NPS_{Prox}I_{45}F_{75}$  depict that a successful self-toss maneuver is possible. The remainder of the maneuvers shown in Figure 10 and Figure 11 are not successful with the FSS colliding and bouncing off the wall barrier or not being propelled sufficiently far away by the actuation of the proximal joint.

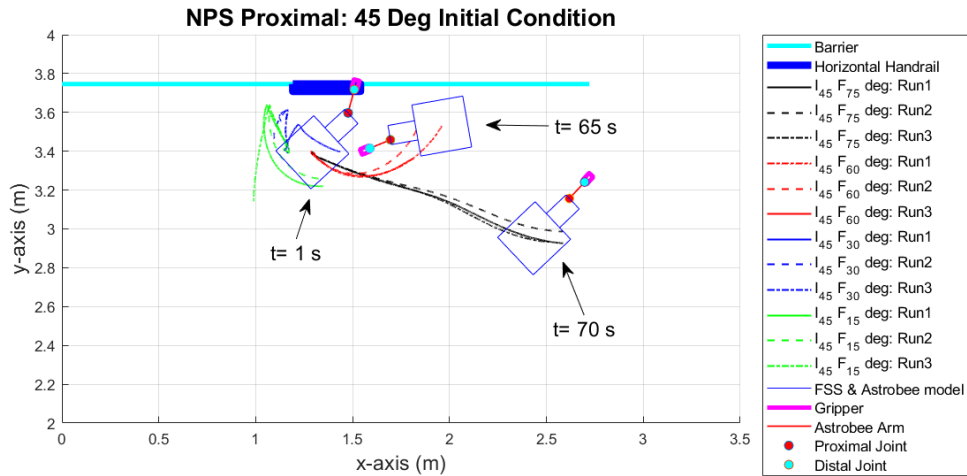
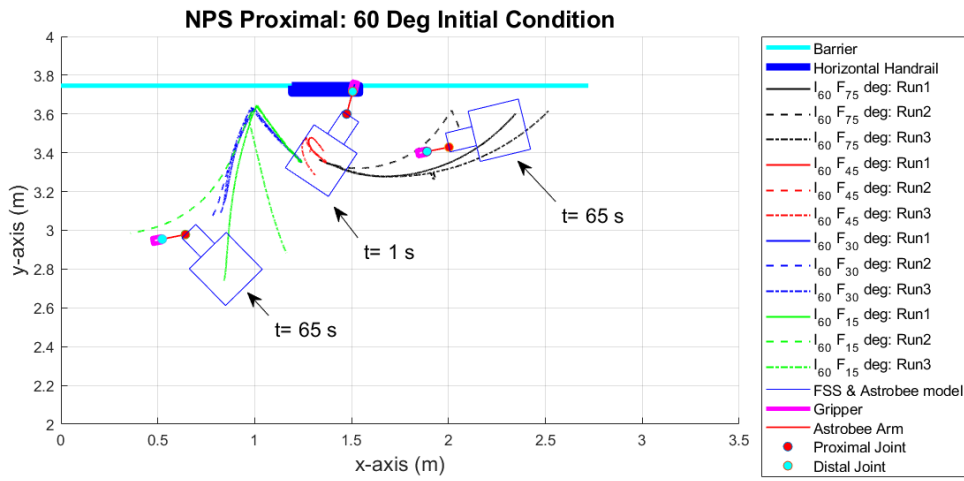


Figure 10:  $NPS_{Prox}I_{45}F_{15,30,60,75}$ , Initial 45 deg to Final Angle: 15, 45, 60, and 75 deg





**Figure 11:  $NPS_{Prox}I_{60}F_{15,30,45,75}$ , Initial 60 deg to Final Angle: 15, 45, 60, and 75 deg**

The NPS proximal experiments in figure 12-14, with initial angle conditions 45, 90, and 135 degrees respectively. From these cases a successful self-toss maneuver was performed by  $NPS_{Prox}I_{45}F_{75,90}$  and  $NPS_{Prox}I_{135}F_{90}$ . With other maneuvers either causing the FSS to bounce into the wall barrier or not traveling a sufficient distance from the FSS initial position.

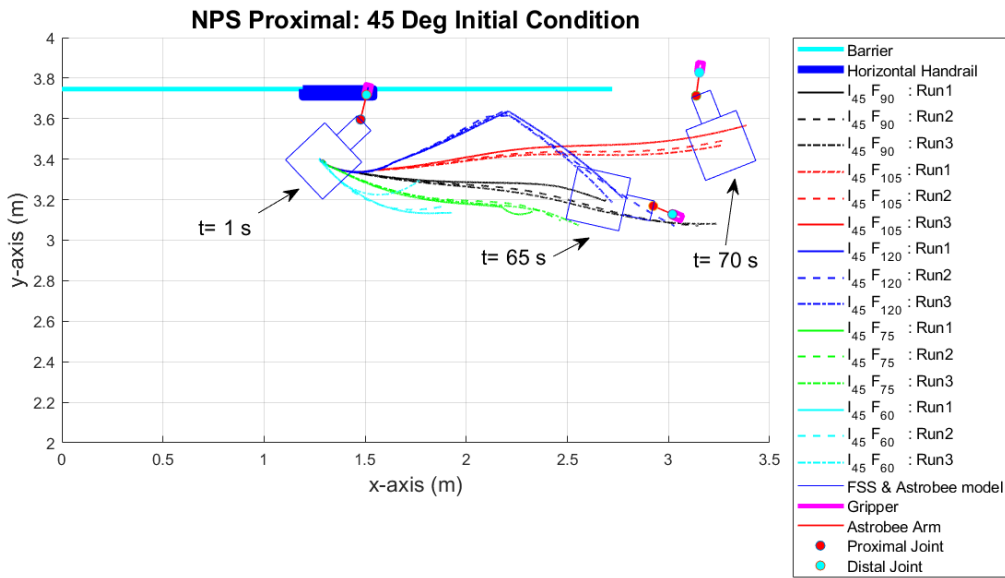


**Figure 12:  $NPS_{Prox}I_{45}F_{90,105,120,75,60}$ , Initial 45 deg to Final Angle: 90, 105, 120, 75 and 60 deg**

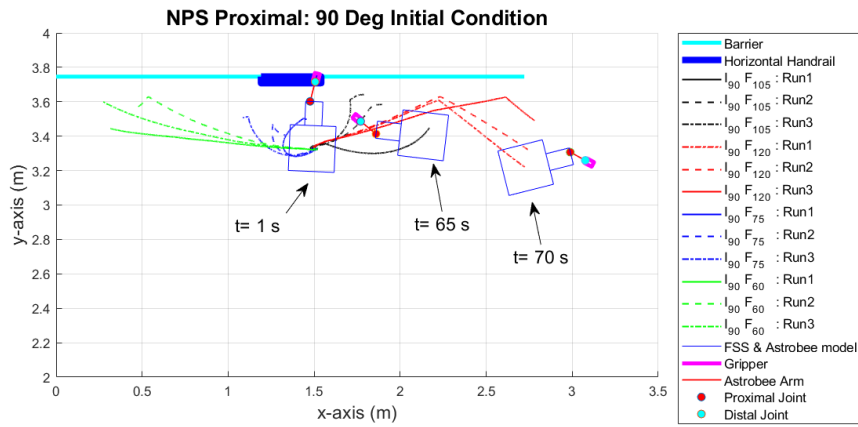


Figure 13:  $NPS_{Prox}I_{90}F_{105,120,75,60}$ , Initial 90 deg to Final Angle: 105, 120, 75, and 60 deg

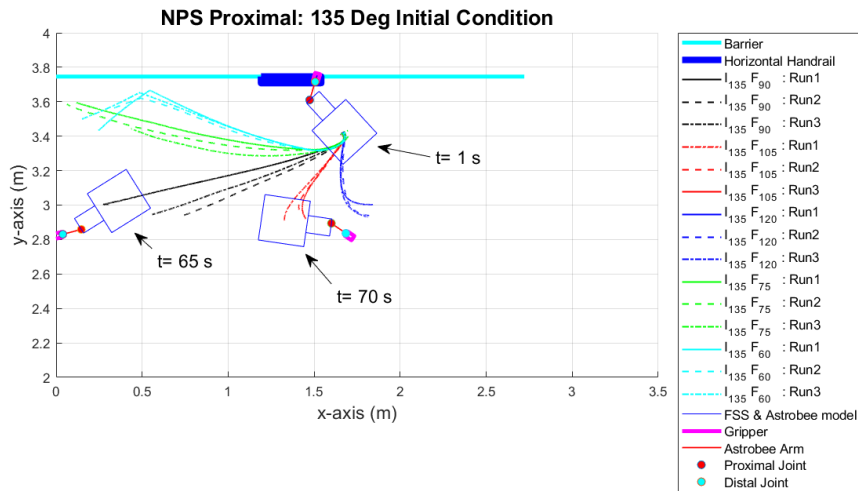


Figure 14:  $NPS_{Prox}I_{135}F_{90,105,120,75,60}$ , Initial 135 deg to Final : 90, 105, 120, 75, and 60 deg

### Self-Toss Distal Experiments Performed at NPS

An example of a distal self-toss experiment at NPS is shown in Figure 15. The FSS starts at the initial angle grasping onto the vertical handrail, from which the distal joint is then commanded to actuate to the final desired angle. Upon reaching the final angle the end-effector is then commanded to release the handrail, allowing the self-toss to occur whereby the FSS launches itself from the handrail.

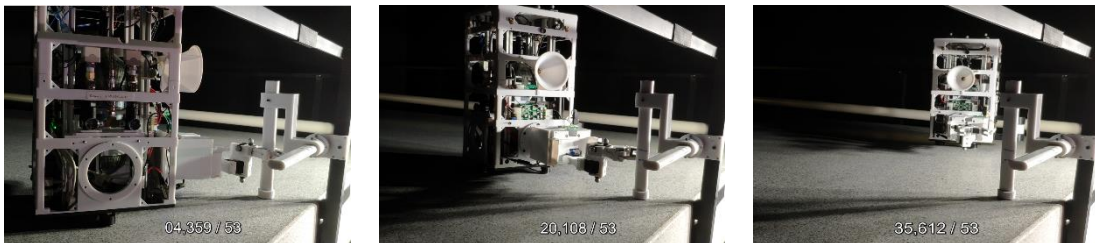


Figure 15: Example B, Distal Self-Toss Maneuver at NPS from vertical handrail

Figure 16 shows the distal experiment ( $45 \text{ deg} \rightarrow -15 \text{ deg}$ ) for the Self-Toss Maneuver where the three runs from the prescribed case were performed, shown in the figure are the three trajectories of each run for the FSS, as well as a depiction of the heading and orientation of the gripper during the self-toss maneuver for Run 1. Similar to the proximal case, the tracking of  $[x, y, \phi]$  for the distal experiment is displayed in Figure 17. The FSS first starts at rest then at the 25 second mark, the distal joint is commanded to actuate with release of handrail from the gripper commanded once the desired final angle is reached.

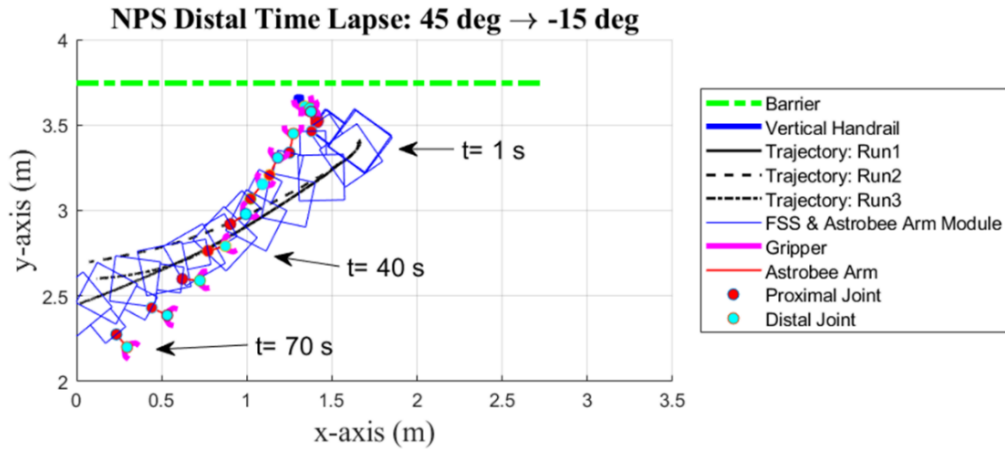


Figure 16: Graph of Distal Self-Toss Maneuver  $45 \rightarrow -15$  Degrees

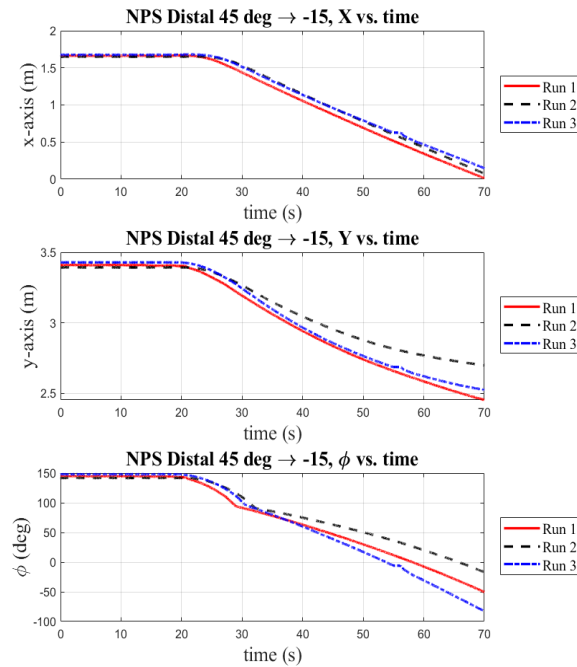


Figure 17:  $[x, y, \phi]$  of the FSS during the Self-Toss Distal Maneuver  $45 \rightarrow -15$  Degrees

## NPS Distal Experiments

Figure 18, 19, and 20 are the NPS distal experiments were performed to evaluate the self-toss maneuver using the actuation of the distal joint. Similar to previous plots, each graph shows the dynamic motion of the FSS during the self-toss maneuver from gripping the handrail to the trajectory after release. The  $NPS_{Dist}I_{45}F_{0,-15,-30}$ ,  $NPS_{Dist}I_{-45}F_{-15,0}$ , and  $NPS_{Dist}I_{45}F_{15}$  show a successful self-toss maneuver, whereby the FSS is able to travel in a consistent trajectory over three separate runs without impacting the barrier or stagnating.

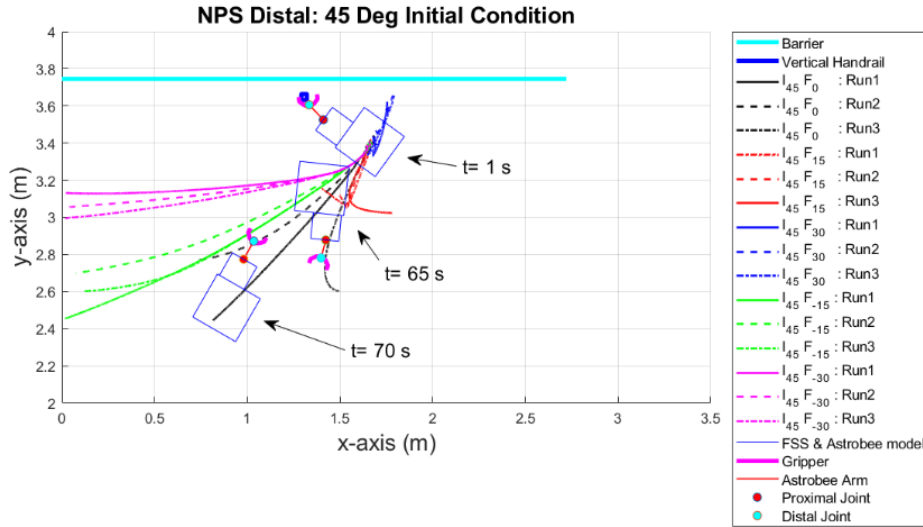


Figure 18:  $NPS_{Dist}I_{45}F_{0,15,30,-15,-30}$ , Initial 45 deg to Final Angle: 0, 15, 30, -15 and 30 deg

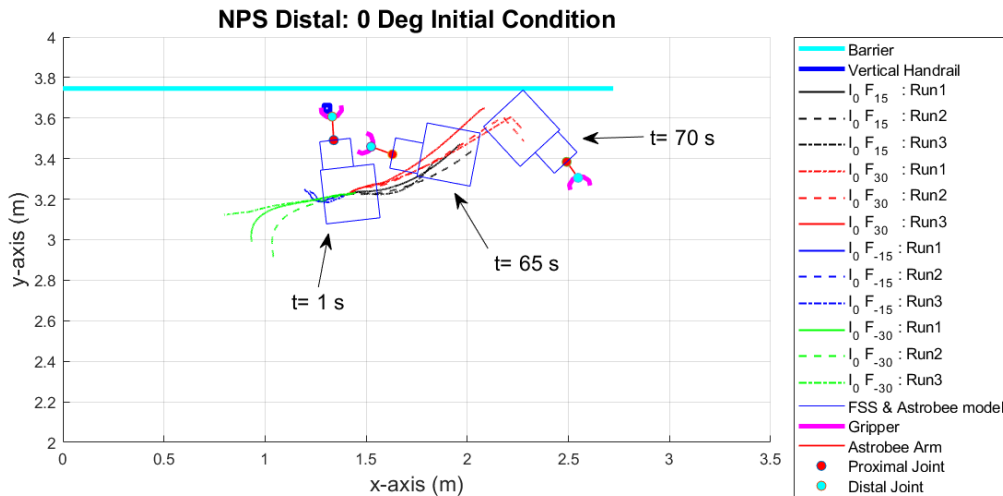


Figure 19:  $NPS_{Dist}I_0F_{15,30,-15,-30}$ , Initial 0 deg to Final Angle: 15, 30, -15 and -30 deg

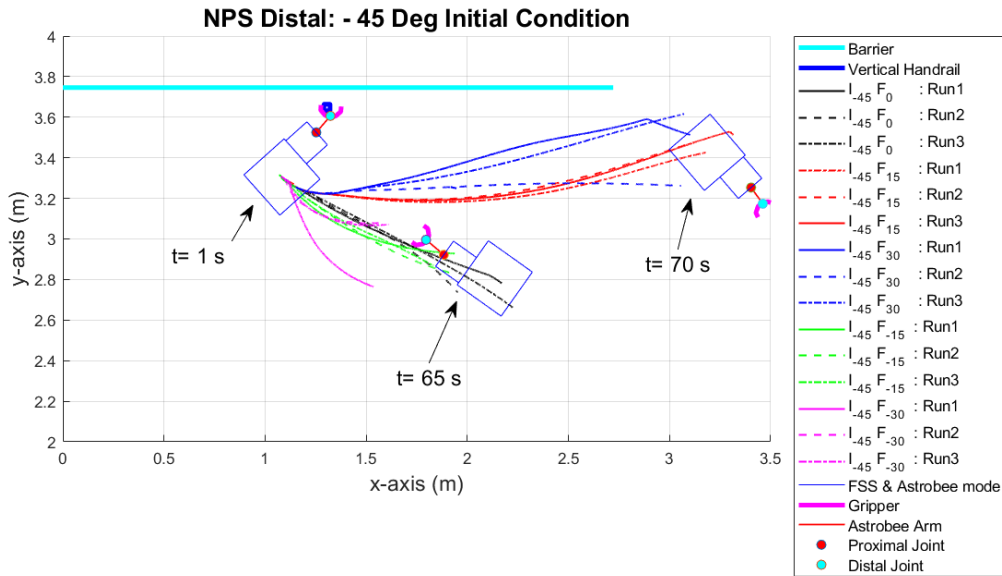


Figure 20:  $NPS_{Dist}I_{-45}F_{0,15,30,-15,-30}$ , Initial – 45 deg to Final: 0, 15, 30, –15 and – 30 deg

### NASA Ames Proximal Experiment

Figure 21 is a series of pictures that showcase the dynamic motion of a self-toss maneuver performed at NASA Ames with the Astrobee Free-Flyer from the 45 to 75 degree position. Astrobee initially was made to grasp the handrail, then the operator sent a command for the Proximal Joint to actuate and upon reaching the goal angle the gripper end-effector was commanded to release. Similar to the NPS experiments three runs were collected for each case.



Figure 21: Astrobee Vehicle at Ames During Self-Toss Maneuver 45 → 75 degrees

### NASA Ames Proximal Self-Toss Experiments

The NASA Ames Astrobee self-toss maneuvers in figure 22, 23, and 24 depict the experimental runs that have been performed. Each graph is grouped by initial angle of the Proximal joint of 45, 90, and 135 degrees respectively with final angles varying from 60 to 120 degrees as described by Table 1. Proximal joint positions and maneuvers greater than 90 degrees are beyond the stated range limit of motion of the Astrobee robotic arm \*, however self-toss maneuvers were performed to compare the dynamic motion of the Astrobee free flyer at NASA Ames versus the FSS vehicle

\* <https://github.com/nasa/astrobee/wiki/Command-Dictionary>

with Astrobee Module at the Naval Postgraduate School. From Figure 22 the Astrobee free flyer is shown to have a stable self-toss maneuver, where  $Ames_{Prox}I_{45}F_{60}$ ,  $Ames_{Prox}I_{45}F_{75}$  and  $Ames_{Prox}I_{45}F_{90}$ .

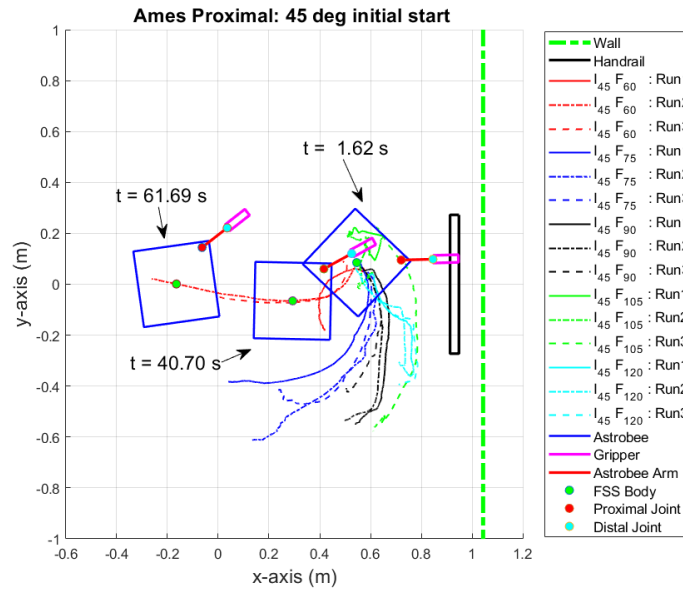


**Figure 22:  $Ames_{Prox}I_{45}F_{60,75,90,105,120}$ , Initial 45 deg to Final: 60, 75, 90, 105 and 120 deg**

Figure 23 the self-toss maneuvers of  $Ames_{Prox}I_{90}F_{60,90}$  as compared to  $Ames_{Prox}I_{90}F_{105,120}$  depict a preferential in the counterclockwise direction due to the distance traveled. This could be because of the relative motion of the center of mass of Astrobee as compared to the proximal joint when grasping the handrail before release. The self-toss maneuvers in Figure 24 have an initial start angle of 135 degrees and actuation of the proximal joint through 120 to 60 degrees final angle, where the Astrobee free-flyer dynamic motion is consistent during the self-toss. Unfortunately, an initial start angle of 135 degrees is outside normal operational command\*.

\* <https://github.com/nasa/astrobee/wiki/Command-Dictionary>

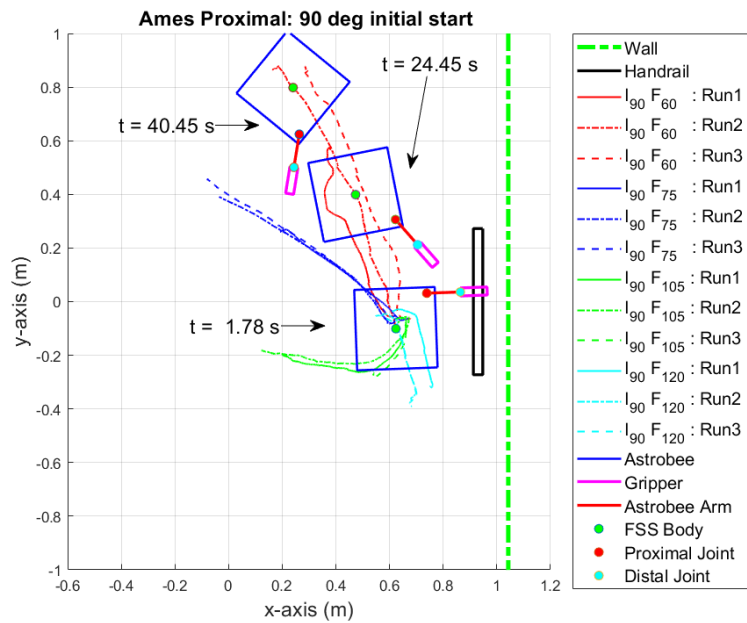


Figure 23:  $Ames_{Prox}I_{90}F_{60,75,105,120}$ , Initial 90 deg to Final Angle: 60, 75, 105, and 120 deg

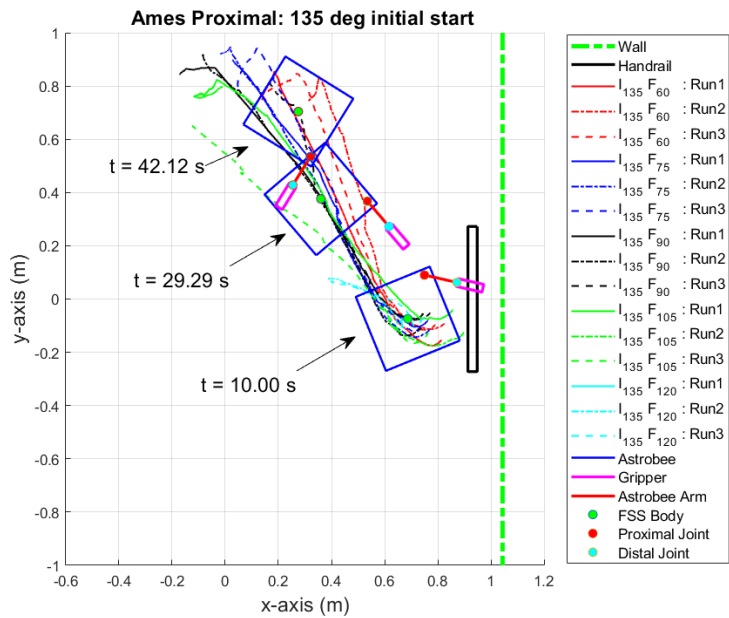
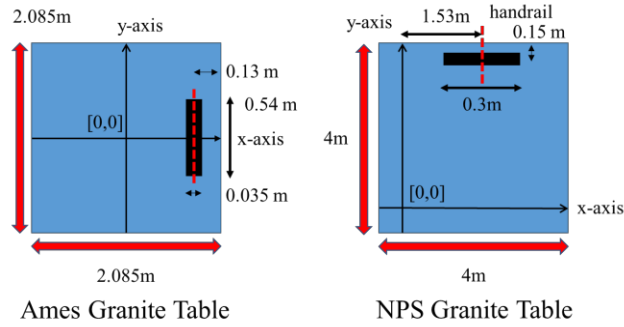


Figure 24:  $Ames_{Prox}I_{135}F_{60,75,90,105,120}$ , Initial 135 deg to Final: 60, 75, 90, 105 and 120 deg

### Global Coordinate Frames and Position of Handrail for Proximal Self-Toss Experiments

Illustrated in Figure 25, the NASA Ames Granite table has its global coordinate frame at the center of the table with the horizontal handrail mounted on the right wall. In comparison, the NPS global coordinate frame is defined offset from the bottom left corner of the granite table, with the horizontal handrail mounted on the top wall at 1.53 m offset from the y-axis. Of particular note, the

adjusted Ames and NPS heading,  $\phi$ , was aligned, however due to pre-defined limits, the NPS heading was defined over the period  $[-\pi, +\pi]$  with the NASA Ames dataset defined over  $[0, +2\pi]$ .



**Figure 25: Illustration of NPS and NASA Ames Granite Table Handrail Orientation Dimensions**

**Example A: Comparison of Proximal Self-Toss  $I_{45}F_{75}$  from the NPS and Ames dataset**

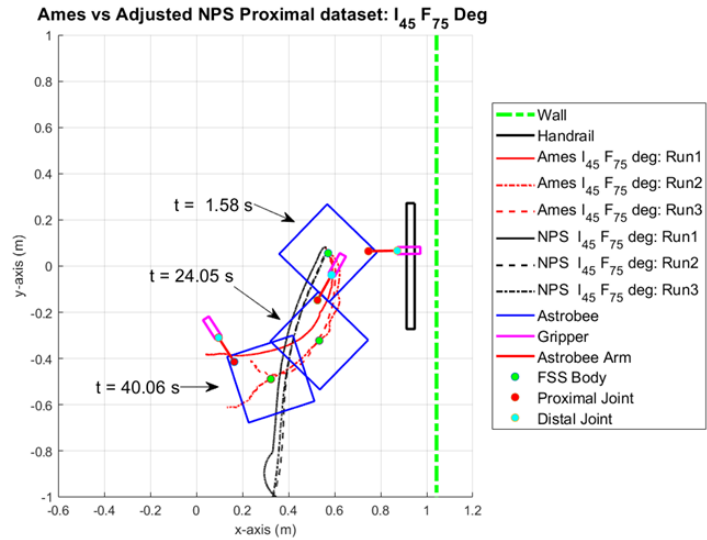


**Figure 26: Comparison of Ames to Adjusted  $NPS_{prox}I_{45}F_{75}$  dataset**

Comparison of self-toss maneuver  $I_{45}F_{75}$  for Ames and NPS dataset is shown in example A with Figure 26 and Figure 27. Whereby the coordinate frame of the NPS dataset was rotated and translated to the Ames coordinate frame in addition to the alignment of initial position, orientation, and time of joint actuation. Thus, allowing for the trajectory of the NPS FSS and the Ames Astrobees Free-Flyer to be plotted and compared against one another. From Figure 26 and Figure 27 both sets of trajectories show the vehicle moving in the same general relative direction with deviation occurring after 30 seconds in the relative x-axis direction. The difference in heading definition from both dataset collections can be seen in the adjusted Ames and NPS  $\phi$  graph in Figure 27.



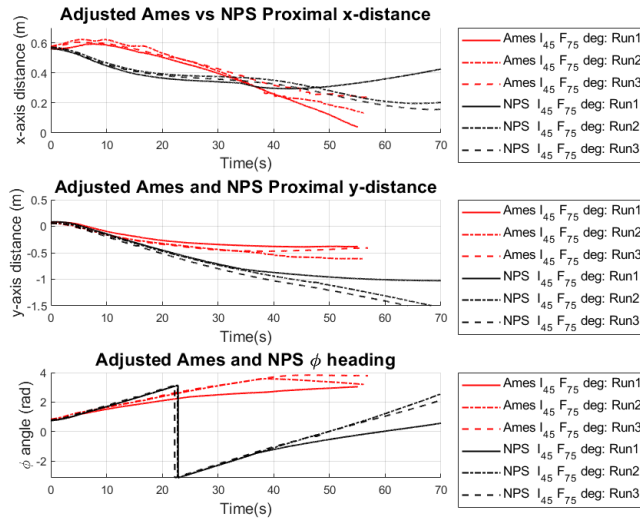


Figure 27: Comparison of  $[x, y, \phi]$  values for proximal experiment  $I_{45}F_{75}$

**Example B: Comparison of Proximal Self-Toss  $I_{135}F_{90}$  from the NPS and Ames dataset**

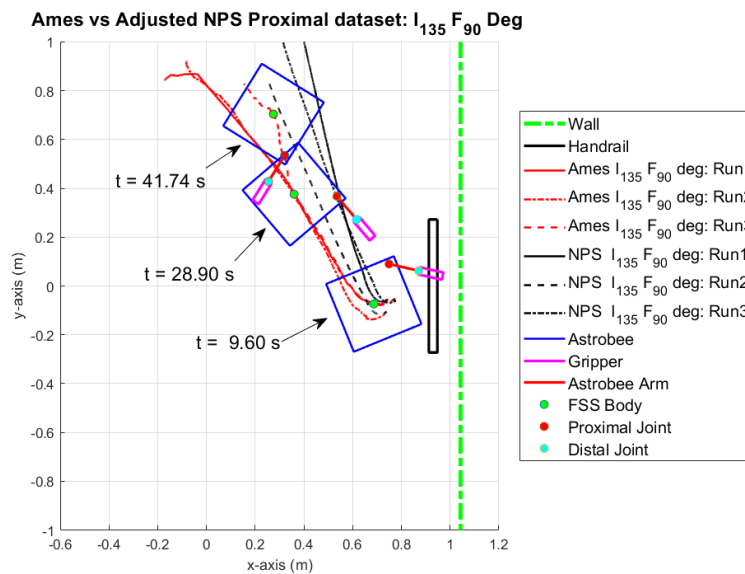
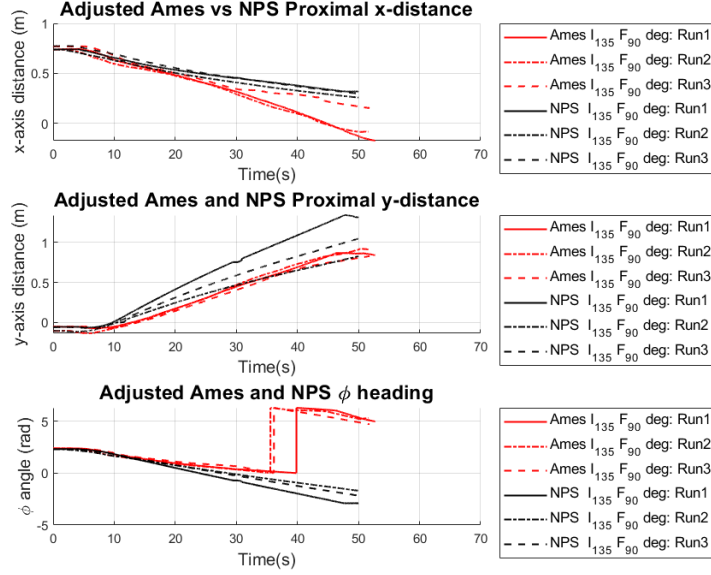


Figure 28: Comparison of Ames to Adjusted  $NPS_{prox}I_{135}F_{90}$  dataset

Similarly for example B, a comparison of the proximal self-toss proximal maneuver  $I_{135}F_{90}$  for the NPS FSS and Ames free-flyer Astrobee is presented in Figure 28 and Figure 29. Where the trajectory of the NPS FSS is compared to that of the Astrobee free-flyer in Figure 28, with the displacement and change in heading,  $\phi$ , shown versus time in Figure 29. From this dataset the vehicles appear to follow similar trajectories and heading, however due to differences in experimental test conditions there does appear to be deviation after the first relative 25 seconds from the moment of release of the end effector from the handrail. The deviation in trajectory could

be caused by difference in mass, inertia, granite surface conditions, and possibly size difference in the NPS FSS and Astrobee Module as compared to the actual Astrobee free-flyer at NASA Ames.



**Figure 29: Comparison of Proximal Self-Toss  $I_{135}F_{90}$  from the NPS and Ames dataset**

### Observations and Discussion

A summary of the self-toss maneuvers utilizing the NPS FSS, and the Astrobee free-flyer at NASA Ames is shown in Table 2 and Table 3.

Table 2 highlights each set of experiments that were completed where the motion of the vehicle during self-toss were defined as either a success in green or failure in orange. A successful self-toss maneuver was defined, if the FSS or Astrobee free-flyer was able to travel in a concise, consistent trajectory, the distance travelled was greater than 30 cm over the initial 50 seconds from gripper release, and the vehicle did not impact the barrier wall during the initial 50 seconds of the maneuver.

Table 3 is a summary of the experiments conducted, where the success and failure of the self-toss maneuver was sorted and presented by the  $\alpha_{diff}$  angle. From equation (1),  $\alpha_{diff}$  was defined as the difference between the initial angle of actuation,  $\alpha_{initial}$ , and the final angle,  $\alpha_{final}$ , during release.

$$\alpha_{diff} = \alpha_{final} - \alpha_{initial} \quad (1)$$

The three categories were defined [ $\alpha_{diff} \leq -30^\circ$ ,  $\alpha_{diff} \geq 30^\circ$ ,  $-30^\circ < \alpha_{diff} < 30^\circ$ ]. Overall trends based on the  $\alpha_{diff}$  were observed: that for the NPS proximal experiments a successful self-toss maneuver was more likely to occur where  $\alpha_{diff} \geq 30^\circ$ , the Ames proximal experiments displayed a strong preference where  $\alpha_{diff} \leq -30^\circ$  led to successful self-toss maneuvers. With the NPS distal experiments outlining that a successful self-toss maneuver was more likely to occur if the difference between initial and final angle was outside the range of  $-30^\circ \leq \alpha_{diff} \leq 30^\circ$ . From Table 2 and the respective graphs, it is interesting to note that a failure of a self-toss maneuver was

also more likely to occur if the  $|\alpha_{diff}|$  angle was larger than  $60^\circ$ , this is because the angle of actuation caused the vehicle to move in a trajectory that was very likely to impact the wall barrier of the experimental setup due to over actuation of the particular joint.

An observation from the NPS and Ames experiments is that there were cases where the FSS vehicle and Astrobee free-flyer displayed a tendency to have an irregular non-smooth trajectory. The non-smooth trajectories could have been due to a variety of reasons such as: the condition of the air-bearing pads, air pressure level during experimental testing, or the presence of particulates on the granite surface. Care was taken to minimize these sources of uncertainty, as well as perform multiple repeats of the each case and test condition, of which the overall trends of the trajectory for the FSS vehicle and Astrobee free-flyer were presented.

**Table 2: Summary of Experimental Results**

NPS		Final Proximal Angle ( $^\circ$ )					NPS		Final Proximal Angle ( $^\circ$ )					Legend
		15	30	45	60	75			60	75	90	105	120	
Initial Proximal Angle ( $^\circ$ )	30	Fail	Fail	Success	Success	Success	Initial Proximal Angle ( $^\circ$ )	45	Success	Success	Success	Success	Success	
	45	Success	Success	Fail	Success	Success		90	Success	Success	Fail	Success	Success	
	60	Success	Success	Success	Fail	Success		135	Success	Success	Success	Success	Success	
NPS		Final Distal Angle ( $^\circ$ )					Ames		Final Proximal Angle ( $^\circ$ )					
		-30	-15	0	15	30			60	75	90	105	120	
Initial Distal Angle ( $^\circ$ )	45	Success	Success	Success	Success	Success	Initial Proximal Angle ( $^\circ$ )	45	Success	Success	Success	Success	Success	
	0	Success	Success	Fail	Success	Success		90	Success	Success	Fail	Success	Success	
	-45	Success	Success	Success	Success	Success		135	Success	Success	Success	Success	Success	

**Table 3: Summary of Self-Toss Experiments based on  $\alpha_{diff} = [\alpha_{final} - \alpha_{initial}]$**

			Success	Fail	Total
Proximal	NPS	$[\alpha_{diff} \geq 30^\circ]$	6	2	26
		$[\alpha_{diff} \leq -30^\circ]$	3	5	
		$[-30^\circ < \alpha_{diff} < 30^\circ]$	2	8	
	AMES	$[\alpha_{diff} \geq 30^\circ]$	2	3	14
		$[\alpha_{diff} \leq -30^\circ]$	5	0	
		$[-30^\circ < \alpha_{diff} < 30^\circ]$	3	1	
Distal	NPS	$[\alpha_{diff} \geq 30^\circ]$	3	2	14
		$[\alpha_{diff} \leq -30^\circ]$	4	1	
		$[-30^\circ < \alpha_{diff} < 30^\circ]$	1	3	

**FUTURE WORK**

A full series comparison of self-toss experiments at NASA Ames and NPS is pending. Additional self-toss Astrobee free flyer maneuvers at NASA Ames would like to be performed in order to supplement the experiments done thus far of the self-toss maneuver utilizing the Astrobee robotic arm. The work being accomplished shall lead to further understanding of the self-toss maneuver in preparation of self-toss validation experiments to be performed on the ISS.

## CONCLUSION

In conclusion, the experiments conducted thus far showcase that self-toss maneuvers utilizing the Astrobee free-flyer robotic arm for proximal and distal actuation respectively is possible. However there does appear to be a range as defined by  $\alpha_{diff}$  where a successful self-toss maneuver is more likely to be achieved due to the initial and final angle of commanded actuation for both the proximal and distal joint respectively. Whereby, based on the experiments conducted for the proximal experiment a  $|\alpha_{diff}| \geq 30^\circ$  for the Ames and NPS datasets, as well as the distal NPS dataset led to a larger likelihood of a successful self-toss maneuver. With limitations found in the proximal datasets that if  $|\alpha_{diff}| \geq 60^\circ$  this would lead to over actuation with the strong possibility that the Astrobee free flyer or FSS vehicle would not be able to complete the maneuver due to impact with the adjacent wall barrier.

## ACKNOWLEDGEMENTS

We would like to thank the assistance and support provided by the Naval Postgraduate School as well as NASA without which this research would not have been possible. We would like to thank the Naval Postgraduate School Foundation for their financial support.

## NOTATION

$\alpha_{diff}$	Actuation angle difference between: $\alpha_{final} - \alpha_{initial}$
$\alpha_{final}$	Actuation angle that the prescribed joint is commanded to move to prior to release of the gripper end-effector
$\alpha_{initial}$	Actuation angle that the prescribed joint is commanded to start at the start of the self-toss maneuver
$Ames_{Prox}I_xF_{a,b,c,...}$	NASA Ames Proximal Dataset with Initial angle $x$ to final angle $a, b, c, \dots$
$FSS$	Floating Spacecraft Simulator
$ISS$	International Space Station
$JAXA$	The Japanese Aerospace Exploration Agency
$MAE$	Mechanical and Aerospace Engineering Department
$NASA$	National Aeronautics and Space Administration
$NPS$	Naval Postgraduate School
$NPS_{Prox}I_xF_{a,b,c,..}$	NPS Proximal Dataset with Initial angle $x$ to final angle $a, b, c, \dots$
$NPS_{Dist}I_xF_{a,b,c,..}$	NPS Distal Dataset with Initial angle $x$ to final angle $a, b, c, \dots$
$POSEIDYN$	Proximity Operation of Spacecraft: Experimental hardware-In-the-loop DYNAMIC simulator

## REFERENCES

- <sup>1</sup> Kwok Choon, S., Chitwood, J., Safbom, C., Leary, P., and Romano, M., "ASTROBATICS: A Hopping-Maneuver Experiment for a Spacecraft-Manipulator System on board the International Space Station," *70th International Astronautical Congress*, Washington, DC: International Astronautical Federation, 2019, pp. 21–25.

- 2 Sayyad, A., Seth, B., and Seshu, P., "Single-legged hopping robotics research—A review," *Robotica*, vol. 25, 2007, pp. 587–613.
- 3 Yoshida, K., "Achievements in space robotics," *IEEE Robotics and Automation Magazine*, vol. 16, 2009, pp. 20–28.
- 4 Upadhyay, S., and Aguiar, A. P., "Local trajectory generation for hopping robots exploring celestial bodies," *AIAA Scitech 2019 Forum*, 2019, pp. 1–12.
- 5 Fiorini, P., and Burdick, J., "The Development of Hopping Capabilities for Small Robots," *Autonomous Robots*, vol. 14, 2003, pp. 239–254.
- 6 Burdick, J., and Fiorini, P., "Minimalist Jumping Robots for Celestial Exploration," *The International Journal of Robotics Research*, vol. 22, Jul. 2003, pp. 653–674.
- 7 Kubota, T., and Yoshimitsu, T., "Intelligent rover with hopping mechanism for asteroid exploration," *2013 6th International Conference on Recent Advances in Space Technologies (RAST)*, 2013, pp. 979–984.
- 8 Yoshimitsu, T., Kubota, T., Adachi, T., and Kuroda, Y., "Advanced robotic system of hopping rovers for small solar system bodies," *International Symposium on Artificial Intelligence, Robotics and Automation in Space*, 2012, pp. 3–7.
- 9 Yoshimitsu, T., Kubota, T., and Nakatani, I., "Operation of MINERVA rover in Hayabusa Asteroid Mission," *57th International Astronautical Congress*, American Institute of Aeronautics and Astronautics, 2006.
- 10 Yoshimitsu, T., Kubota, T., and Nakatani, I., "MINERVA rover which became a small artificial solar satellite," *Proceedings of the Small Satellite Conference*, 2006.
- 11 McCamish, S. B., Romano, M., Nolet, S., Edwards, C. M., and Miller, D. W., "Flight Testing of Multiple-Spacecraft Control on SPHERES During Close-Proximity Operations," *Journal of Spacecraft and Rockets*, vol. 46, 2009, pp. 1202–1213.
- 12 Mitani, S., Goto, M., Konomura, R., Shoji, Y., Hagiwara, K., Shigeto, S., and Tanishima, N., "Int-Ball: Crew-Supportive Autonomous Mobile Camera Robot on ISS/JEM," *2019 IEEE Aerospace Conference*, 2019, pp. 1–15.
- 13 Schmitz, H.-C., Kurth, F., Wilkinghoff, K., Müllerschowski, U., Karrasch, C., and Schmid, V., "Towards Robust Speech Interfaces for the ISS," *Proceedings of the 25th International Conference on Intelligent User Interfaces Companion*, New York, NY, USA: Association for Computing Machinery, 2020, pp. 110–111.
- 14 Bualat, M., Barlow, J., Fong, T., Provencher, C., Smith, T., and Zuniga, A., "Astrobee: Developing a free-flying robot for the international space station," *AIAA SPACE 2015 Conference and Exposition*, 2015, pp. 1–10.
- 15 Vargas, A. M., Ruiz, R. G., Wofford, P., Kumar, V., Van Ross, B., Katterhagen, A., Barlow, J., Flückiger, L., Benavides, J., Smith, T., and Bualat, M., "Astrobee: Current status and future use as an international research platform," *Proceedings of the International Astronautical Congress, IAC*, vol. 2018-October, 2018, pp. 1–8.
- 16 Lee, D. H., Coltin, B., Morse, T., Park, I. W., Flückiger, L., and Smith, T., "Handrail detection and pose estimation for a free-flying robot," *International Journal of Advanced Robotic Systems*, vol. 15, 2018, pp. 1–12.
- 17 NASA Ames Intelligent Robotics Group, *Astrobee Guest Science Guide*, Moffet Field, CA: 2017.
- 18 Flückiger, L., Browne, K., Coltin, B., Fusco, J., Morse, T., and Symington, A., "Astrobee Robot Software: Enabling Mobile Autonomy on the ISS," *Int. Symposium on Artificial Intelligence, Robotics and Automation in Space (i-SAIRAS)*, Madrid, Spain: I-SAIRAS, 2018.
- 19 Alsup, K. P., Virgili-llop, J., Komma, J., and Romano, M., "ANALYSIS AND SIMULATION OF ROBOTIC HOPPING MANEUVERS INSIDE THE INTERNATIONAL SPACE STATION WITH ASTROBEE," *29th AAS/AIAA Space Flight Mechanics Meeting*, Ka'anapali, HI: AAS / AIAA, 2019, pp. 1–20.
- 20 Komma, J. L., "MECHATRONICS: THE DEVELOPMENT, ANALYSIS, AND GROUND-BASED DEMONSTRATIONS OF ROBOTIC SPACECRAFT HOPPING WITH A MANIPULATOR," Monterey, CA; Naval Postgraduate School, 2018.
- 21 Park, I. W., Smith, T., Sanchez, H., Wong, S. W., Piacenza, P., and Ciocarlie, M., "Developing a 3-DOF compliant perching arm for a free-flying robot on the International Space Station," *IEEE/ASME International Conference on Advanced Intelligent Mechatronics, AIM*, 2017, pp. 1135–1141.
- 22 Zappulla II, R., Virgili-Llop, J., Zagaris, C., Park, H., and Romano, M., "Dynamic Air-Bearing Hardware-in-the-Loop Testbed to Experimentally Evaluate Autonomous Spacecraft Proximity Maneuvers," *Journal of Spacecraft and Rockets*, vol. 54, 2017, pp. 825–839.
- 23 Virgili-Llop, J., Drew, J. V., Zappulla, R., and Romano, M., "Laboratory experiments of resident space object capture by a spacecraft–manipulator system," *Aerospace Science and Technology*, vol. 71, Dec. 2017, pp. 530–545.
- 24 Wilde, M., Clark, C., and Romano, M., "Historical survey of kinematic and dynamic spacecraft simulators for laboratory experimentation of on-orbit proximity maneuvers," *Progress in Aerospace Sciences*, 2019, p. 100552.